J Fluoresc (2014) 24:1827–1840
DOI 10.1007/s10895-014-1471-3

ORIGINAL PAPER

Phenalenone Fluorophores-Synthesis, Photophysical Properties and DFT Study

Kiran R. Phatangare · Sandip K. Lanke · Nagaiyan Sekar

Received: 30 July 2014 / Accepted: 29 September 2014 / Published online: 5 October 2014

Abstract Three new fluorescent phenalenone derivatives incorporating bexozazolyl, benzothiazolyl and benzimidazolyl rings have been synthesized from the intermediate 3-(1,3-benzazol-2-yl) naphthalen-2-ol by reacting with glycerol. The synthesized phenalenone derivatives were well characterized by using FT-IR, ^{1}HNMR, ^{13}CNMR and Mass spectroscopy. The photophysical properties of these phenalenone derivatives show that these dyes absorb in the range of 300–429 nm and emitted in the range of 348–578 nm. The relative fluorescence quantum yields of these derivatives were determined by using fluorescein, tinopal and anthracene as the reference standards. Photophysical properties of the synthesized phenalenone dyes were evaluated by UV-Visible spectroscopy and compared with the computed vertical excitations obtained from TD-DFT. Thermal stability of the compounds were studied by using thermo gravimetric analysis and results show that compounds are thermally stable up to 298–347 °C.

Keywords 3-(1,3-benzazol-2-yl) naphthalen-2-ol · Phenalenone · Density functional theory · Photophysical study

Introduction

Phenalenone is an aromatic ketone whose chemical structure is given in (Fig. 1). The family of phenalenes and phenalenones constitutes an unusual class of non benzenoid aromatic compounds which have attracted considerable attention because of the remarkable stability of phenalenyl radicals, anions, and cations [1, 2]. They rarely occur in nature. Recently a number of oxygenated derivatives of phenalenones have been isolated from plants, fungi and several of these compounds have been found to exhibit interesting photophysical properties [3]. The phenalenone derivatives with electron-donor and electron-acceptor substituents display a high sensitivity to the polarity of the local environment, and their spectroscopic behavior is susceptible to the physicochemical properties of surrounding environment [4]. Therefore, they have found application in a number of areas including fluorescent probes and markers for cells [5]. Phenalenone derivatives find application as a fluorescent chemosensor for fluoride anion with high sensitivity and selectivity [6]. Phenalenone is a universal standard for the determination of quantum yields of singlet oxygen O_2 ($^{1}\Delta_g$) [7, 8]. Phenalenone is a very efficient and unique photosensitizer that can generate $^{1}O_2$ with a quantum yield of close to unity in most of the solvent ranging from water to benzene [7, 9] and hence it is used as a fluorescent probe for singlet oxygen sensor [10]. It would acts as a $^{1}O_2$ photosensitizers [11].

There are a number of reports describing the isolation and structural identification of 9- and 4-substituted phanalenones [12, 13]. The photophysical properties of phenalenones are studied widely [1, 7, 14, 15].

Keeping in mind the interesting properties of phenalenone fluorophores, it was envisaged to obtain structures with high quantum yield, dual emission with red shifts by proper substitution in the phenalenone core. Such molecules will be of great interest in the development of new photosentizers or chemosensors. In continuation of our previous work [16, 17], in this paper we report the synthesis of bezimidazolyl, bnzoxazolyl and benzothiazolyl substituted phenalenones, their photophysical properties and a DFT approach to their photophysical properties.

K. R. Phatangare · S. K. Lanke · N. Sekar (✉)
Tinctorial Chemistry Group, Institute of Chemical Technology, N. P. Marg, Matunga, Mumbai 400 019, Maharashtra, India
e-mail: n.sekar@ictmumbai.edu.in

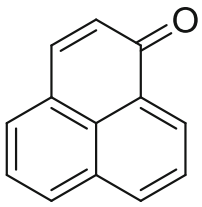

Fig. 1 Chemical Structure of Phenalenone

Results and Discussion

Chemistry

The synthetic scheme for the preparation of benzoxazolyl-benzo[f]chromen-3-one derivatives is shown in Scheme 1. 3-(1,3-Benzoxazol-2-yl) naphthalen-2-ol **2** was prepared by the reported procedure, from 3-hydroxynaphthalene-2-carboxylic acid **1** and 2-aminophenol **2** in presence of PCl_3 in chlorobenzene at 130–135 °C [18, 19], while 3-(1,3-benzothiazol-2-yl) naphthalen-2-ol **3** was prepared by reported procedure from 3-hydroxynaphthalene-2-carboxylic acid **1** and 2-aminothiophenol in presence of PCl_3 in toluene at 111–114 °C [20]. (1,3-Benzimidazol-2-yl) naphthalen-2-ol **4** was prepared by the reaction of 3-hydroxynaphthalene-2-carboxylic acid **1** with benzene-1,2-diamine in presence of polyphosphoric acid at 130-135 °C for 2 h [21]. The synthesized compounds were characterized by FT-IR, ^{1}H-NMR and mass spectral analysis. The molecular ion peak at 261.95 and 271 and 260.2 confirms the formation of compound 2, 3 and 4 respectively.

The novel fluorescent phenalenone derivatives **5**–**7** were synthesized from the intermediate 3-(1,3-benzazol-2-yl) naphthalen-2-ol **2**–**4** by reacting it with glycerol in presence of ferrous sulphate, boric acid phosphoric acid, and 4-nitrobenzenesulphonic acid sodium salt for at 150–155 °C [22, 23] for respective time as mentioned in the experimental section. The purity of the compounds was checked by TLC using precoated silica gel as stationary phase, using appropriate solvent system as mobile phase and visualized under UV-light. The structures of the synthesized compounds were confirmed by FT-IR, ^{1}H-NMR and mass spectrometry. The absence of broad IR peak at 3,010 cm^{-1} confirms that –COOH of 3-hydroxynaphthalene-2-carboxylic acid was converted to oxazole ring structure. Also the IR peak at 1,585, 1,477 cm^{-1} confirms the formation of –C = N of oxazole ring formation and the peak at 1720–1,735 cm^{-1} corresponds to the carbonyl stretching frequency. The compounds **5**, **6** and **7** show molecular ion peak 298.4, 314.3 and 294 which corresponds to M+ 1 peak of compounds **5**, **6** and **7** respectively.

Reagent and conditions:a) X = O, chlorobenzene/ PCl_3, 4 h, X = S, xylene, PCl_3, 6 h, X = NH, PPA, 3.5 h. b) Glycerol, phosphoric acid, boric acid, ferrous sulphate, p-nitrobenzene sulfonic acid sodium salt, heated at 150–155 °C.

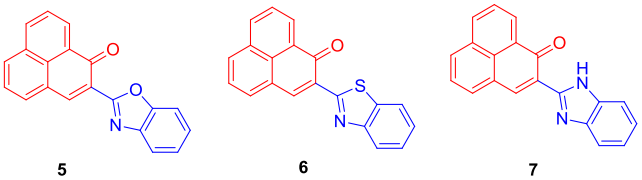

5 6 7

Photophysical and Computational Study of Compound 5

To evaluate the effect of solvent polarity on absorption-emission properties of the synthesized compounds, the compounds **5**–**7** were tested in different solvents of varying polarity and hydrogen bonding capability. Various polar and non polar solvents were tested for the effect of solvent on their absorption-emission characteristics.

The compound **5** shows two distinct absorption peaks, one around at 300 nm and another around at 415 nm along with

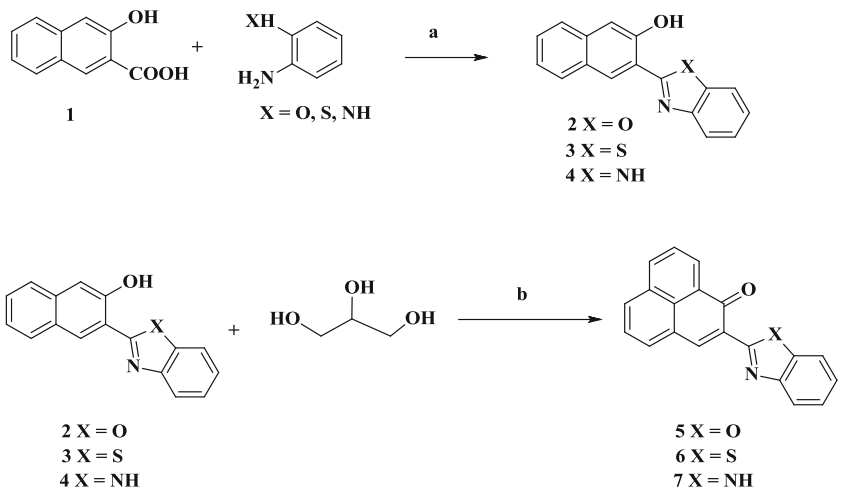

Scheme 1 Synthesis of 3-(1,3-benzazol-2-yl)naphthalen-2-ol and its phenalenone derivatives

shoulder peak at 369 nm in all the solvents. For the short wavelength absorption wavelength, higher molar absorptivity of 19691.1 L mol^{-1} cm^{-1} was observed in DMF while in the case of long wavelength absorption wavelength it is 19780.2 L mol^{-1} cm^{-1} in toluene (Table 1). The compound **5** shows hyperchromic effect in the case of non-polar solvents (Fig. 2a). The largest difference between the computed and experimental absorption maxima was 10 nm in DMF for the short wavelength region. In the case of long wavelength region it is 54 nm in toluene. In case of DMF the computed vertical excitation at 307 nm with oscillator strength of 0.4466 obtained from sixth excited state corresponds to the absorption at shorter wavelength (297 nm). FMO 77 and 78 was found to be HOMO and LUMO respectively. The vertical excitation obtained in excited state 2 at 364 nm with oscillator strength of 0.1514 corresponds to shoulder peak at 366 nm (Table 1). The vertical excitation presented in (Fig. 1, SI) for methanol solvent states that the excitation at 307 nm is because of HOMO to LUMO+1 transition which shows the contribution of 68 %, responsible for absorption at 300 nm. The HOMO-LUMO transition is responsible for experimental absorption at 414 nm and absorption at 329 nm is due HOMO-1 to LUMO transition (Table 1). Similar trend was observed for other solvents except toluene wherein HOMO-2→LUMO transition is obtained from fourth excited state which is responsible for shoulder peak at 369 nm.

Table 1 Observed UV-visible absorption and vertical excitation of compound **5** in different solvents.[a]

Solvent	Experimental[b]		Exc λ (nm)	TD-DFT[c]			
	Abs λ (nm)	Molar absorptivity (a) L mol^{-1} cm^{-1}		Vertical Excitation		*f*	Assignment
				nm	eV		
MeOH	300	15919.2	276	307	4.0438	0.4357	H→L+1 (68 %)[d]
	369	12652.2		362	3.4080	0.1447	H-1→L (66 %)[e]
	414	15948.9		456	2.7183	0.3522	H→L (69 %)[f]
CH_3CN	297	17998.2	274	307	4.0419	0.4374	H→L+1 (68 %)[d]
	366	13216.5		364	3.4071	0.1462	H-1→L (66 %)[e]
	411	17523.0		456	2.7171	0.3553	H→L (69 %)[f]
DMF	297	19691.1	284	307	4.0329	0.4466	H→L+1 (68 %)[d]
	366	13840.2		364	3.4016	0.1514	H-1→L (67 %)[e]
	411	17102		458	2.7092	0.3713	H→L (69 %)[f]
DMSO	300	14434.2	276	307	4.0339	0.4450	H→L+1 (68 %)[d]
	372	12058.2		364	3.4026	0.1513	H-1→L (67 %)[e]
	414	16305.3		457	2.7110	0.3691	H→L (69 %)[f]
DCM	300	19305.0	278	307	4.0376	0.4484	H→L+1 (68 %)[d]
	366	12325.5		365	3.3978	0.1358	H-1→L (65 %)[e]
	411	16424.1		459	2.7005	0.3684	H→L (69 %)[f]
$CHCl_3$	300	18740.7	276	307	4.0389	0.4527	H→L+1 (68 %)[d]
	369	13572.9		366	3.3881	0.1059	H-1→L (61 %)[e]
	417	18354.6		461	2.6883	0.3701	H→L (69 %)[f]
EtOAc	300	15147.0	278	307	4.0449	0.4442	H→L+1 (68 %)[d]
	363	12143		365	3.3958	0.1125	H-1→L (61 %)[e]
	408	15830.1		459	2.6994	0.3579	H→L (69 %)[f]
Toluene	300	12336.4	298	307	4.0379	0.4606	H→L+1 (67 %)[d]
	369	12266.1		362	3.4229	0.1196	H-2→L (55 %)*
	411	19780.2		465	2.6648	0.3743	H→L (69 %)[f]

[a] Analysis were carried out at room temperature (25 °C)

[b] Experimentally observed λ_{max}

[c] TD-DFT computations were carried out with the use of optimized structures at B3LYP method with 6-31G(d) basis set

[d] Only major contributions are presented from excited state 6

[e] Only major contributions are presented from excited state 3

[f] Only major contributions are presented from excited state 1

*Only major contributions are presented from excited state 4; *f*=Oscillator strength

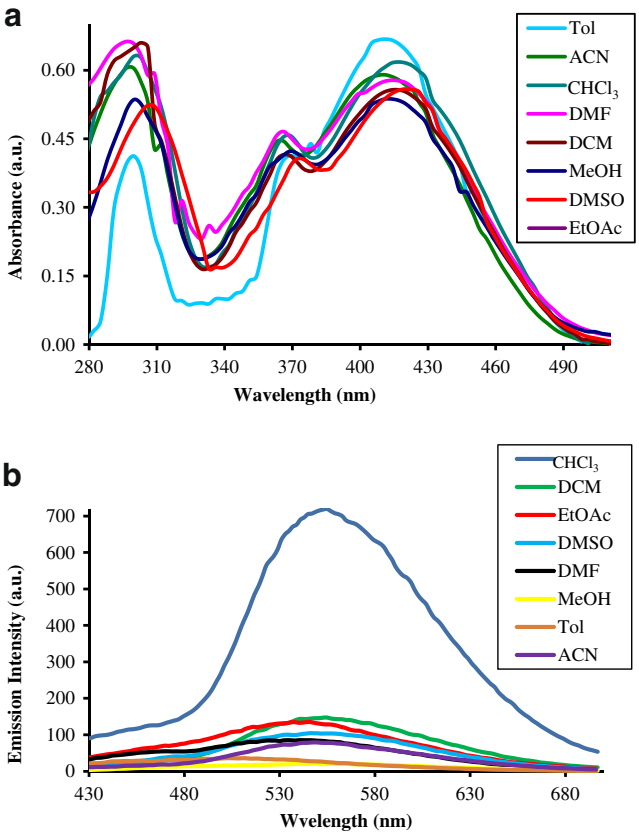

Fig. 2 **a** Absorption spectra of compound 5 in different solvents. **b** Fluorescence spectra of compound 5 in different solvents

The compound **5** emits in the range of 511 nm to 554 nm with the Stokes shift range of 100 to 136 nm (Table 2). The compound **5** shows the highest emission intensity (Fig. 2b) in chloroform solvent with the highest fluorescence quantum yield (Φ=0.166). In toluene slight blue shift of 37 nm was observed as compared to methanol. Except chloroform the fluorescence emission intensity was very less resulting in less quantum yield which varies from 0.038 to 0.085 in other solvents (Fig. 3).

Table 2 Observed Emission of compound **5** in various solvents and its quantum yield.[a]

Solvent	λ_{abs}^{max} [b] (nm)	λ_{ems}^{max} [c](nm)	Stokes Shift nm (cm^{-1})	ϕ_f[d]
MeOH	414	548	134(5906)	0.038
ACN	411	547	136(6049)	0.073
DMF	411	543	132(5914)	0.065
DMSO	414	547	133(5873)	0.067
DCM	411	554	143(6280)	0.073
$CHCl_3$	417	554	137(5930)	0.166
EtOAc	408	546	138(6194)	0.085
Toluene	411	511	100(4761)	0.042

[a] Analysis were carried out at room temperature (25 °C)

[b] Absorption wavelength maxima

[c] Fluorescence emission maxima

[d] Fluorescein was used as reference standard for quantum yield calculations

Photophysical and Computational Study of Compound 6

Irrespective of solvent polarity the compound **6** shows two distinct absorption peaks at 315 and 429 nm (Fig. 4a) along with a shoulder peak at 342 nm. Neither red nor blue shift was observed in acetonitrile, but it shows the slightly hyperchromic shift with highest molar absorptivity of 16635.2 L mol^{-1} cm^{-1}. The absorption ranges from 315 to 327 nm at shorter wavelength while for longer wavelength it ranges from 429 to 432 nm. The absorption at shorter wavelength shows higher molar absorptivity than longer wavelength.

For the compound **6** the largest difference between the experimental and computed absorption was found to be only 12 nm in case of DMSO for shorter absorption. In the other solvents the computed absorption maxima were very close to the experimental observation.. The electronic transition from HOMO to LUMO +1 originating from excited state contributed 68 % and corresponds to the experimentally observed λ_{max} at around 315 nm in methanol, acetonitrile, DMF, DMSO and DCM. In other solvents like chloroform, ethyl acetate and toluene the same transition is originated from the excited state 7 with comparable oscillator strength from 0.4299 to 0.4581. In all the solvents the prominent absorption can be assigned to HOMO to LUMO (69 % contribution) with oscillator strength range of 0.3320-0.3516 (Table 3).

The compound **6** emits from 348 to 578 nm with dual emission in all the solvents except in methanol (it shows blue shifted emission). In all the solvents it shows good fluorescence (Fig. 4c). The Stokes shift varies from 33 nm to 99 nm for short wavelength emission and 103–263 nm in case of long wavelength emission. In methanol the compound **6** shows anomalous behavior than the other solvents. Both the shorter and longer emission peaks are slightly blue shifted. Compound 6 shows the blue shifted emission of 315 and 418 nm. In toluene compound 6 shows blue shift of 31 nm as compared to DMSO, while the largest red shift in second emission was observed for DCM (Fig. 4b, Table 4).

In the case of chloroform and ethyl acetate the compound **6** shows the highest emission intensity attributed to the highest quantum yield of 0.171 and 0.189 respectively. The quantum yield for shorter emission and longer emission were calculated separately by using tinopal and fluorescein as reference standards respectively for all the solvents under the consideration for study. The quantum yield for shorter emission was found to be higher than the longer emission. Summation of both the quantum yield gives total quantum yield for compound 6 (Table 4) [24]. The excitation spectra were plotted in (Fig. 2, SI).

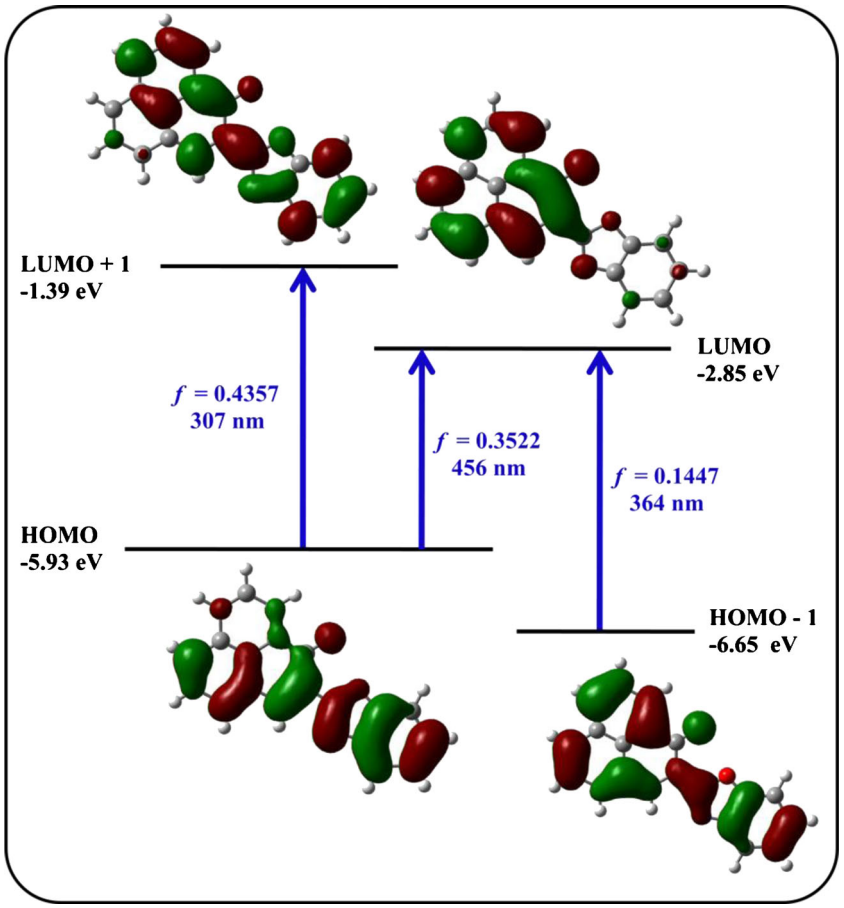

Fig. 3 Representation of the UV-visible absorption (vertical excitation) compound **5** in methanol[a]. [a]The vertical excitation related calculations were based on optimized ground state geometry and the emission calculations were based on optimized excited state geometry at B3LYP/6-31G(d). The energy level of HOMO and LUMO at excited state are different than at the ground state

Photophysical and Computational Study of Compound 7

In similar line of the compounds 5 and 6, compound **7** also shows two distinct absorption peaks, but the shoulder peak around 366 is the promising peak (Fig. 5a). The compound **7** shows the λ_{max} absorption around 306–312 nm, longer wavelength absorption at 423 nm to 462 nm and shoulder peak at 364 nm to 369 nm with considerable molar absorptivity (9139.6-11455.8 L mol^{-1} cm^{-1}). The highest molar absorptivity of 25916.4 L mol^{-1} cm^{-1} was observed in case of DCM while lowest was observed for chloroform (20376.3 L mol^{-1} cm^{-1}).

A largest difference of 4 nm between experimental and computed absorption is observed for DMSO and DCM in short wavelength absorption while in the case of long wavelength absorption it is 15 nm in chloroform solvent. The FMO 77 and 78 was found to be HOMO and LUMO respectively in all the solvents. The vertical excitation HOMO to LUMO+1 at 307 to 311 nm with the contribution of 65 % corresponds to the experimentally observed λ_{max} at 306 to 312 nm which originates from excited state 6 for polar solvents. For non polar solvents like DCM, $CHCl_3$, ethyl acetate and toluene the same transition was originates from excited state 7. The electronic transitions from HOMO-2 to LUMO and HOMO-1 to LUMO are responsible for the absorption at 364 to 399 nm and 432–464 nm in all solvents (Table 5).

The emission properties of the compound **7** were somewhat different than the compound **5** and **6**. The compound **7** shows two different absorption peaks upon excitation at two different absorption wavelengths. The excitation at around 310 nm leads to the emission at 334–394 nm (Fig. 5b) while the excitation at 370 nm leads to the emission at 411–431 nm (Fig. 5c). The excitation at 370 nm leads to the same type of emission pattern observed at 310 nm. The Stokes shift for the first and the second emission varies from 28 to 78 nm and 32 to 65 nm which is less than the first one (Table 6).

Excitation at 310 nm compound **7** shows highest emission intensity in methanol (Fig. 5b) leads to the highest quantum yield of 0.117 while in chloroform it was 0.101. When the compound **7** was excited at 369 nm in chloroform it shows emission at 431 nm with increasing emission intensity. For the other solvents quantum yield varies from 0.045-0.096 and 0.020-0.062 nm for short and long wavelength emission respectively (Table 6).

Effect of Viscosity on Compound 6

The effect of increasing the concentration of glycerol on the fluorescence intensity of the novel synthesized substituted phenalenone gains very high importance. To understand the effect of viscosity on the absorption and emission intensities

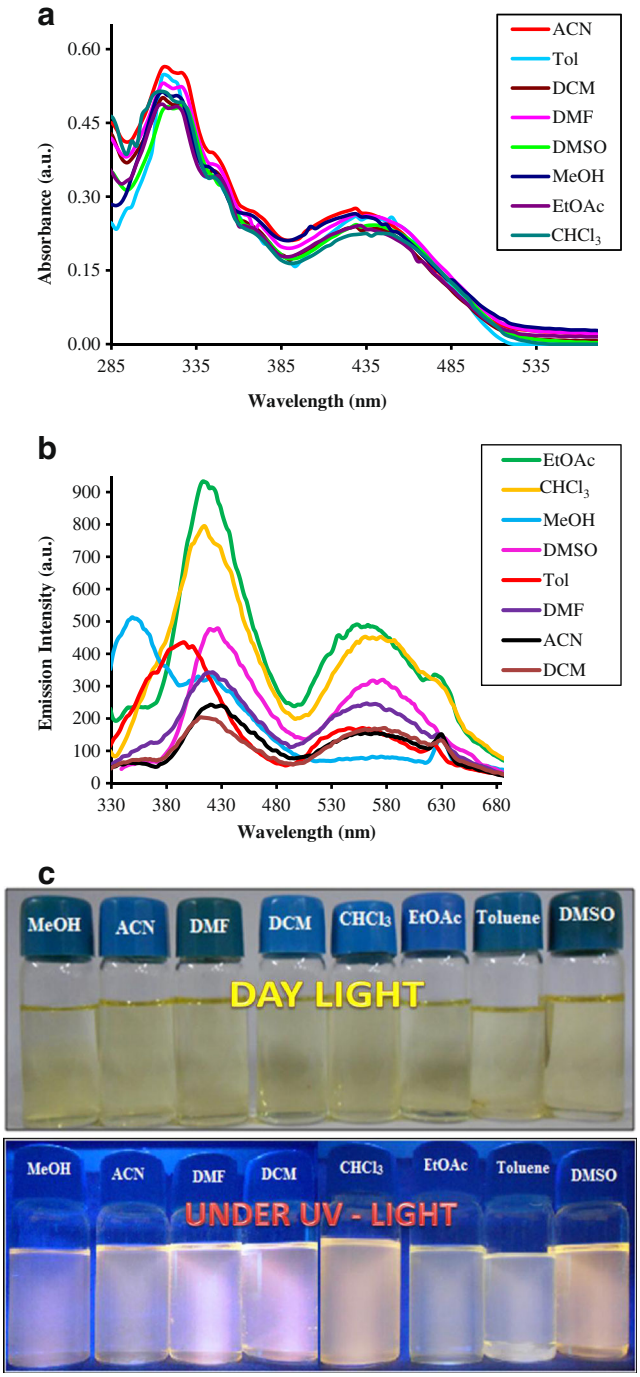

Fig. 4 **a** Absorption spectra of compound **6** in different solvents. **b** Fluorescence spectra of compound **6** in different solvents. **c** Daylight and UV light photographs of compound 6

of compound **6** its absorption and emission properties in presence of different viscous solution of glycerol were studied. Figure 6a clearly indicates that the absorption intensity for both peaks, shorter and longer absorption peaks goes on decreasing as viscosity increases. Similar behavior was observed for the emission spectra. As viscosity increases emission intensity decreases hence we can conclude that compound 6 shows aggregation quenching effect (Figs. 6b, and 7).

There are two possible rotamers in each compound. In "Rotamer a" the pending benzazole ring nitrogen is closer towards carbonyl oxygen while in "Rotamer b" benzazolyl oxygen is closer to the carbonyl oxygen (Fig. 8). The Table 7 for ground state stability of each compound **5**–**7** states that the "Rotamer b" for all compound **5**–**7** is more stable than "Rotamer a". The "Rotamer b" for all compound **5**–**7** was optimized in eight different solvents for which solvatochromism study was performed. The optimized structures of all synthesized compounds **5**–**7** in methanol are presented in Fig. 9.

The dihedral angle between the two rings (phenalenone and benzazole ring) is zero confirms that the optimized structure is planer and the point group for all the optimized structure is Cs (Center of symmetry). The bond length C9-O22 is 1.233 Å, 1.239 Å and 1.244 Å for rotamer **5b**, **6b** and **7b** respectively.

The distance between phenalenone and benzazole ring (Bond length C8-C14) is 1.465 Å which is same for both rotamer **6b** and **7b** while it is 1.462 Å in rotamer **5b**. The distance C14-O34, C14-S34 and C14-N34 was found to be 1.375 Å, 1.784 Å and 1.374 Å respectively. The bond angle C14-O34-C17 and C14-N34-C17 was found to be 104.5° and 105° for **5b** and **7b** respectively while C14-S34-C17 bond angle was found to be 88.5° for **6b**.

Thermogravimetric Analysis

To investigate the thermal stability of synthesized compounds **5**–**7** thermal stability study has been carried out using thermo gravimetric analysis (TGA) technique. The thermal gravimetric analysis has been carried out over temperature range of 50–600 °C under nitrogen atmosphere. TGA analysis curves of all compounds (**5**–**7**) as shown in Fig. 10 and Table 8 indicates that the stability of all compounds varies from 298 to 347 °C. Amongst these compounds compound **6** is less stable than the other two compounds. Compound **7** shows good thermal stability up to 347 °C (838 %). After that it starts to decompose, up to 600 °C it decomposes almost completely. Compound **6** is 95.78 % stable up to 298 °C. Same is the case with compound **5**, it is 91.43 % stable up to 321 °C. After that it decomposed very fast and up to 375 °C it decomposes 70 %. Up to 600 °C all compounds decomposes completely. The comparison of T_d (decomposition temperature) showed that the thermal stability of the compound **5**–**7** decreases in the order **7**>**5**>**6** as shown in Table 8.

Experimental Section

Materials and Methods

All the commercial reagents and solvents were purchased from S. D. Fine Chemicals (India) and Sigma Aldrich and

Table 3 Observed UV-visible absorption and vertical excitation of compound **6** in different solvents.[a]

Solvent	Experimental[b]		Exc λ (nm)	TD-DFT[c]			
	Abs λ (nm)	Molar absorptivity (a) L mol^{-1} cm^{-1}		Vertical Excitation		*f*	Assignment
				nm	eV		
MeOH	315	15244.0	317	315	3.9416	0.4135	H→L+1 (68 %)[d]
	342	10685.6		365	3.3950	0.1982	H-2→L (68 %)[e]
	429	78844.0		465	2.6659	0.3320	H→L (69 %)[f]
ACN	315	16635.2	276	315	3.9398	0.4151	H→L+1 (68 %)[d]
	345	11514.4		365	3.3937	0.1989	H-2→L (68 %)[e]
	429	8169.6		465	2.6649	0.3353	H→L (69 %)[f]
DMF	315	15688.0	284 308	315	3.9317	0.4248	H→L+1 (68 %)[d]
	348	10685.6		366	3.3869	0.2027	H-2→L (68 %)[e]
	429	7814.4		467	2.6575	0.3516	H→L (69 %)[f]
DMSO	327	14385.6	358	315	3.9325	0.4228	H→L+1 (68 %)[d]
	345	10093.6		366	3.3878	0.2020	H-2→L (68 %)[e]
	429	7192.8		466	2.6595	0.3496	H→L (69 %)[f]
DCM	315	14829.6	274	315	3.9372	0.4316	H→L+1 (68 %)[d]
	345	10448.8		366	3.3884	0.2050	H-2→L (68 %)[e]
	429	7074.4		469	2.6441	0.3447	H→L (69 %)[f]
$CHCl_3$	315	15214.4	276	315	3.9395	0.4411	H→L+1 (67 %)[*]
	345	10064.0		366	3.3882	0.2084	H-2→L (68 %)[e]
	429	6600.8		472	2.6277	0.3423	H→L (69 %)[f]
EtOAc	315	14444.8	278	314	3.9444	0.4299	H→L+1 (67 %)[*]
	348	10123.2		365	3.3933	0.2039	H-2→L (68 %)[e]
	432	7133.6		470	2.6404	0.3319	H→L (69 %)[f]
Toluene	315	16161.6	306	315	3.9395	0.4581	H→L+1 (67 %)[*]
	345	10123.2		366	3.3871	0.2149	H-2→L (68 %)[e]
	429	7696.0		475	2.5957	0.3423	H→L (69 %)[f]

[a] Analysis were carried out at room temperature (25 °C)

[b] Experimentally observed λ_{max}

[c] TD-DFT computations were carried out with the use of optimized structures at B3LYP method with 6-31G(d) basis set

[d] Only major contributions are presented from excited state 6

[e] Only major contributions are presented from excited state 4

[f] Only major contributions are presented from excited state 1

[*] Only major contributions are presented from excited state 7; *f*=Oscillator strength

were used without purification. The reaction was monitored by thin layer chromatography using 0.25 mm silica gel 60 F_{254} precoated plates (Merck), which were visualized under UV light. Melting point was recorded by open capillary on Sunder Industrial Product and is uncorrected. The FT-IR spectra were recorded on FTIR-8400S SHIMADZU spectrophotometer. 1H-NMR spectra were recorded on a VXR 400-MHz instrument using trimethylsilane as an internal standard (VARIAN). Mass spectra were recorded on Finnigan Mass spectrometer (EI). The visible absorption spectra of the compounds were recorded on a Perkin-Elmer Lambda 25 UV-Visible spectrometer. Fluorescence emission spectra were recorded on Varian Cary Eclipse fluorescence spectrophotometer using freshly prepared solutions. DSC-TGA measurements were performed on SDT Q 600 v8.2 Build 100 model of TA instruments Waters (India) Pvt. Ltd. Purification of all the compounds was generally achieved by re-crystallization technique.

Computational Details

The various conformers of the coumarins **5** to **7** and their tautomers involved are illustrated in Fig. 8. The ground state (S_o) geometry of the conformers and tautomers of all these compounds in their C_s symmetry were optimized in the gas phase using Density Functional Theory (DFT) [25]. The functional used was B3LYP. The B3LYP method combines Becke's

Table 4 Observed emission of compound **6** in various solvents and its quantum yield.[a]

Solvent	λ_{abs}^{max}[b] (nm)	λ_{ems}^{max}[c] (nm)	Stokes Shift nm (cm^{-1})	ϕ_f[d]	Total Quantum Yield ϕ_f[d]
MeOH	315	348	33(3010)	0.078	0.098
		418	103(7822)	0.020	
ACN	315	420	105(7936)	0.076	0.101
		560	245(13888)	0.025	
DMF	315	422	107(8049)	0.065	0.116
		562	247(13952)	0.051	
DMSO	327	427	100(7161)	0.077	0.139
		577	250(13250)	0.062	
DCM	315	410	95(7355)	0.089	0.145
		578	263(14444)	0.056	
$CHCl_3$	315	414	99(7591)	0.101	0.171
		560	245(13888)	0.070	
EtOAc	315	414	99(7591)	0.112	0.189
		552	237(13630)	0.077	
Toluene	315	396	81(6493)	0.069	0.124
		558	243(13824)	0.055	

[a] Analysis were carried out at room temperature (25 °C)

[b] Absorption wavelength maxima

[c] Fluorescence emission maxima

[d] Tinopal and fluorescein was used as reference standard at shorter and longer wavelength respectively for quantum yield calculations

three parameter exchange functional (B3) [26] with the nonlocal correlation functional by Lee, Yang and Parr (LYP) [27]. The basis set used for all atoms was 6-31G (d), the latter has been justified in the literature [28, 29] for the current investigation. The vibrational frequencies at the optimized structures were computed using the same method to verify that the optimized structures correspond to local minima on the energy surface. The vertical excitation energies at the ground-state equilibrium geometries were calculated with TD-DFT [30–32]. The low-lying first singlet excited state (S_1) of each conformer was relaxed using the TD-DFT to obtain its minimum energy geometry. The difference between the energies of the optimized geometries at the first singlet excited state and the ground state was used in computing the emissions [33]. The frequency computations were also carried out on the optimized geometry of the low-lying vibronically relaxed first excited state of the conformers. All the computations in solvents of different polarities were carried out using the Polarizable Continuum Model (PCM) [34, 35]. All the electronic structure computations were carried out using the Gaussian 09 program [36].

Experimental Procedure for Synthesis of Compounds 2–7

3-(Benzo[d]oxazol-2-yl)naphthalen-2-ol (2)

A mixture of 2-aminophenol (1.09 g, 0.01 mol) and 3-hydroxynaphthalene-2-carboxylic acid **1** (1.88 g, 0.01 mol)

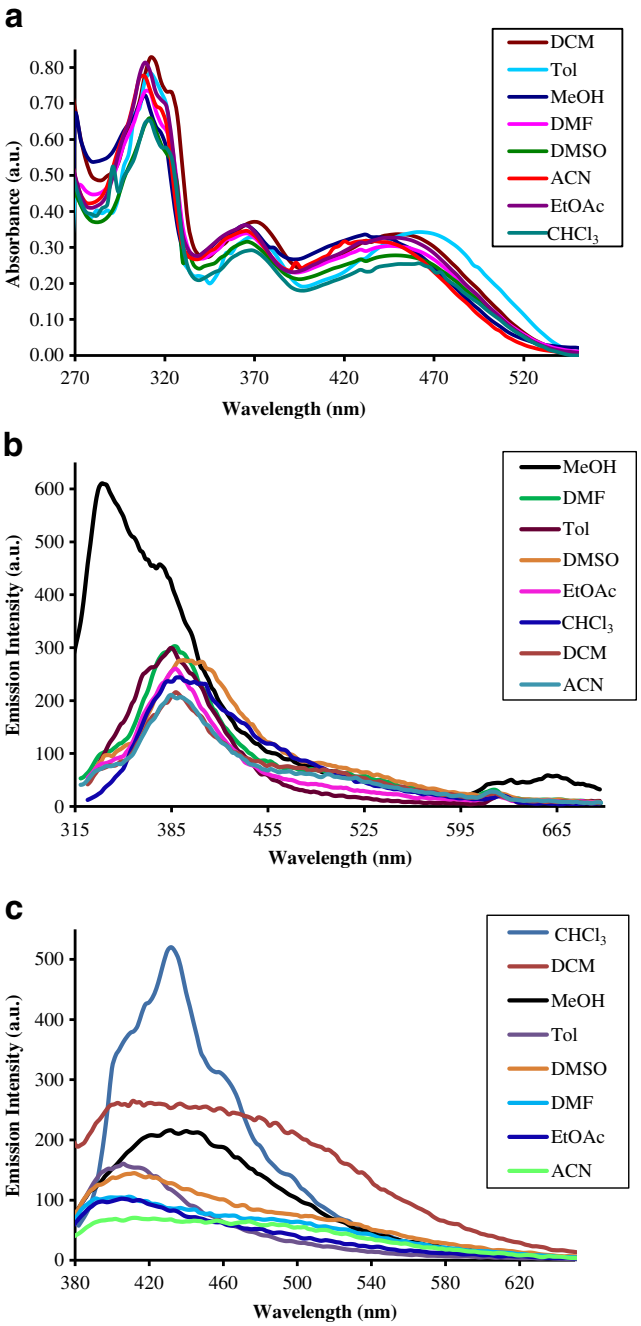

Fig. 5 **a** Absorption spectra of compound **7** in different solvents. **b** Fluorescence spectra of compound **7** in different solvents at ~310 nm excitation. **c** Fluorescence spectra of compound **7** in different solvents at ~370 nm excitation

were refluxed (133–135 °C) in chlorobenzene (10 mL) in presence of PCl_3 (Ueno R. et al. 2004) (2 g, 1.3 mL, 0.01 mol) for 4 h. After completion of reaction, the solid product was precipitated out and was filtered to get crude product **2**. Yield 2.06 g (79 %) which was further recrystallized form ethanol, mp: 171–173 °C (Lit. mp: 171-172 °C) [19].

Table 5 Observed UV-visible absorption and vertical excitation of compound **7** in different solvents.[a]

Solvent	Experimental[b]		Exc λ (nm)	TD-DFT[c]			
	Abs λ (nm)	Molar absorptivity (a) L mol^{-1} cm^{-1}		Vertical Excitation		*f*	Assignment
				nm	eV		
MeOH	306	21878.7	280	307	4.0392	0.5942	H→L+1 (65 %)[d]
	366	11299.3		366	3.3900	0.2091	H-2→L (69 %)[e]
	432	10516.8		434	2.8555	0.0158	H-1→L (70 %)[f]
CH_3CN	309	24555	276	307	4.0376	0.5973	H→L+1 (65 %)[d]
	366	10829.8		366	3.3884	0.2105	H-2→L (69 %)[e]
	444	11735		434	2.8567	0.0159	H-1→L (70 %)[f]
DMF	309	22974.2	284	308	4.0284	0.6134	H→L+1 (65 %)[d]
	366	10610.7	304	367	3.3804	0.2178	H-2→L (69 %)[e]
	447	9515.2		434	2.8568	0.0165	H-1→L (70 %)[f]
DMSO	312	20626.7	304	308	4.0303	0.6107	H→L+1 (65 %)[d]
	366	9890.8	334	367	3.3816	0.2166	H-2→L (69 %)[e]
	447	8701.4		434	2.8597	0.0164	H-1→L (70 %)[f]
DCM	312	25916.4	276	308	4.0211	0.6178	H→L+1 (65 %)*
	366	11455.8		367	3.3806	0.2182	H-2→L (69 %)[e]
	450	10548.1		440	2.8159	0.0166	H-1→L (70 %)[f]
$CHCl_3$	312	20376.3	276	309	4.0093	0.6268	H→L+1 (65 %)*
	369	9139.6		367	3.3781	0.2206	H-2→L (69 %)[e]
	462	14272.8		447	2.7722	0.0170	H-1→L (70 %)[f]
EtOAc	309	25478.2	278	308	4.0214	0.6114	H→L+1 (65 %)*
	366	11299.3		366	3.3851	0.2140	H-2→L (69 %)[e]
	447	10235.1		444	2.7916	0.0164	H-1→L (70 %)[f]
Toluene	312	24539.2	302	311	3.9845	0.6420	H→L+1 (65 %)*
	364	10266.4		368	3.3728	0.2243	H-2→L (69 %)[e]
	462	10735.9		460	2.6948	0.0178	H-1→L (70 %)[f]

[a] Analysis were carried out at room temperature (25 °C)

[b] Experimentally observed λ_{max}

[c] TD-DFT computations were carried out with the use of optimized structures at B3LYP method with 6-31G(d) basis set

[d] Only major contributions are presented from excited state 6

[e] Only major contributions are presented from excited state 4

[f] Only major contributions are presented from excited state 2

*Only major contributions are presented from excited state 7;=Oscillator strength

*3-(Benzo[d]thiazol-2-yl)naphthalen-2-ol (**3**)*

Phosphorus trichloride (4.13 g (2.6 mL), 0.03 mol) was added drop wise to a mixture of the 3-hydroxynaphthalene −2-carboxylic acid **1** (6.2 g, 0.033 mol) and 2-aminothiophenol (4.0 g, (3.85 mL), 0.036 mol) in toluene (50 mL). Slight exotherm was observed. Temperature was maintained below 45–50 °C during the addition of phosphorus trichloride. The mixture was boiled vigorously under reflux for 4 h, whereupon the cooled solution was made alkaline using 20 % sodium carbonate solution. Solid was obtained which filtered and purified using methanol followed by 80 % aqueous acetone wash to get compound **3** ((Yield 2.00 g (72 %)), mp: 180–182 °C (Lit. mp: 182–183 °C) [20].

3-(1H-Benzo[d]imidazol-2-yl)naphthalen-2-ol (4)

A mixture of benzene-1,2-diamine (1.08 g, 0.01 mol) and 3-hydroxynaphthalene-2-carboxylic acid **1** (1.88 g, 0.01 mol) were heated at 130–135 °C in stirrable amount of polyphosphoric acid (5 g) for 2 h. After completion of reaction the tarry reaction mass was cooled to room temperature and slowly added to the

Table 6 Observed emission of compound **7** in various solvents and its quantum yield.[a]

Solvent	λ_{abs}^{max}[b] (nm)	λ_{ems}^{max}[c] (nm)	Stokes Shift nm (cm^{-1})	ϕ_f[d]
MeOH	306	334	28(2739)	0.117
	366	431	65(4120)	0.062
ACN	309	384	75(6320)	0.045
	366	411	45(2991)	0.020
DMF	309	368	59(5188)	0.091
	366	408	42(2812)	0.034
DMSO	312	394	82(6670)	0.066
	366	411	45(2991)	0.045
DCM	312	388	76(6278)	0.063
	366	411	45(2991)	0.081
$CHCl_3$	312	390	78(6410)	0.051
	369	431	62(3898)	0.101
EtOAc	309	388	79(6589)	0.065
	366	405	39(2631)	0.021
Toluene	312	384	72(6009)	0.096
	369	405	36(2408)	0.053

[a] Analysis were carried out at room temperature (25 °C)

[b] Absorption wavelength maxima

[c] Fluorescence emission maxima

[d] Anthracene and tinopal was used as reference standard at shorter and longer wavelength for quantum yield calculations

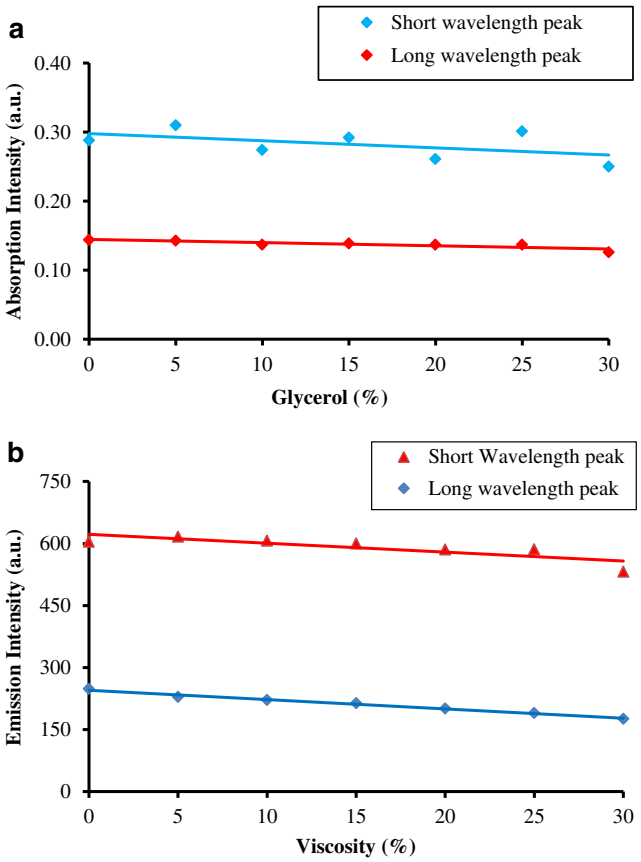

Fig. 6 **a** Plot of absorption intensity against % Glycerol in DMF. **b** Plot of emission intensity against % Glycerol in DMF

crushed ice. Solid product was precipitated out and was filtered and washed well with water to get crude product **4**. Yield 1.95 g (75 %) which was further recrystallized form ethanol, mp: 267–270 °C, decomp. (Lit. mp: 268–272 °C, decomp [21].

2-(benzo[d]oxazol-2-yl)-1H-phenalen-1-one derivatives from phosphoric acid (5)

A mixture of 3-(benzo[*d*]oxazol-2-yl)naphthalen-2-ol (1 g, 1 eq.), p-nitrobenzene sulfonic acid sodium salt (0.86 g, 1 eq.), glycerol (5.21 g, 15 eq.), ferrous sulphate (0.21 g, 0.2 eq.) and boric acid (0.3 g, 1.3 eq.) was heated at 150–155 °C in presence of phosphoric acid (10 mL) for 120 min. Reaction progress was monitored by TLC. After completion of reaction, allowed to cool to room temperature. It was slowly quenched to crushed ice. Final compound was extracted with ethyl acetate. Ethyl acetate layer was dried over sodium sulphate and concentrated to get crude product. Further crude product was recrystallized from ethyl alcohol. Crude yield= 63 %, M. P=225-229 °C.

FT-IR 3040 (Aromatic -CH Stretching), 1728 (C=O stretching) 1577, 1450, (C=C, C=N ring stretching), 1244, 1101 (C-O stretching), 862, 739 (Aromatic -CH out of plane bending) cm^{-1}.

^1H NMR ($CDCl_3$, 300 MHz) δ=7.26 (dd, *J*=2.2, 7.9 Hz, 1H, Ar-H), 7.36 (dd, *J*=8.2 Hz, 1H, Ar-H), 7.40 (d, *J*=1.5 Hz, 1H, Ar-H), 7.66-7.69 (m, *J*=2.6, 7.5 Hz, 2H, Ar-H), 7.84-7.89 (dd, *J*=1.8, 7.2 Hz, 2H, Ar-H), 8.17 (m, 2.7, 7.9 Hz, 1H, Ar-H),

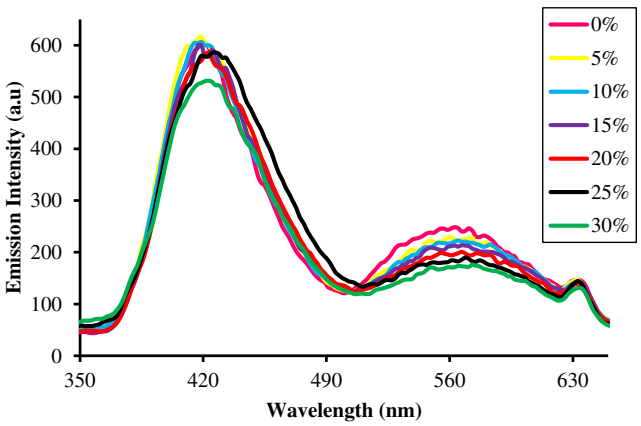

Fig. 7 Effect of viscosity on emission of compound **6**

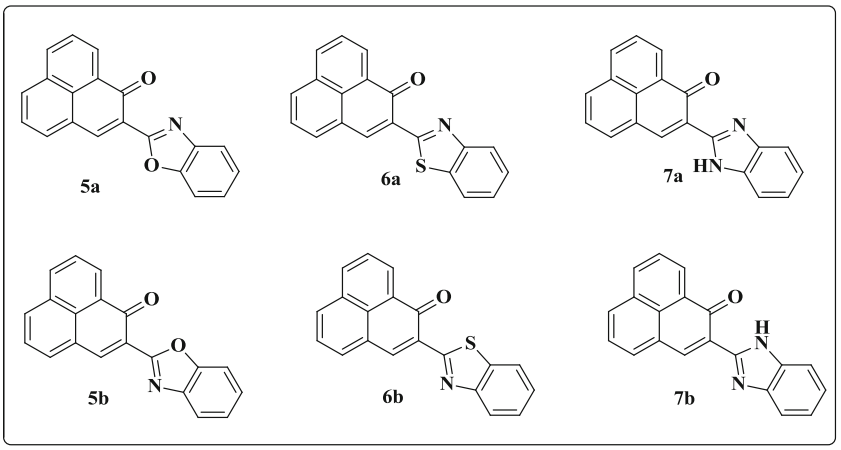

Fig. 8 The possible rotamers of compounds of **5**–**7**

8.25-8.28 (m, 2.3, 8.6 Hz, 2H, Ar-H), 8.82 (d, *J*=2.9, 7.3 Hz, 1H, Ar-H) ppm.

^{13}C NMR ($CDCl_3$, 75 MHz) δ=110.7, 120.4, 124.6, 125.5(s), 127.0 (s), 126.5 (s), 127.7 (s), 131.6 (s), 132.0, 133.7(s), 135.1 (s), 144.6 (s), 162.5 ppm.

MS (*m*/*z*): 298.4 (M+1 ion peak)

2-(benzo[d]thiazol-2-yl)-1H-phenalen-1-one derivatives from phosphoric acid (6)

A mixture of respective 3-(benzo[*d*]thiazol-2-yl)naphthalen-2-ol (1 g, 1 eq.), p-nitrobenzene sulfonic acid sodium salt (0.86 g, 1 eq.), glycerol (5.21 g, 15 eq.), ferrous sulphate (0.21 g, 0.2 eq.) and boric acid (0.3 g, 1.3 eq.) was at 150–155 °C heated in presence of phosphoric acid (10 mL) for 120 min. Reaction progress was monitored by TLC. After completion of reaction, allowed to cool to room temperature. It was slowly quenched to crushed ice. Final compound was extracted with ethyl acetate. Ethyl acetate layer was dried over sodium sulphate and concentrated to get crude product. Further crude product was recrystallized from ethyl alcohol. Crude yield= 67 %, M.P = >300 °C

^{1}H NMR: (DMSO-d_6, 300 MHz) δ=7.40-7.56 (m, *J*=2.9, 7.2, 8.4 Hz, 3H, Ar-H), 7.83-7.88 (t, *J*=2.5, 8.9 Hz, 2H, Ar-H), 7.98-8.19 (m, *J*=1.9, 2.7, 7.2 Hz, 2H, Ar-H), 8.43 (m, *J*= 2.2, 8.3 Hz, 1H, Ar-H), 7.56 (d, *J*=2.4, 8.4 Hz, 1H, Ar-H), 8.74-8.85 (d, 2.5, 8.6 Hz, 2H, Ar-H) ppm.

^{13}C NMR: (DMSO-d_6, 75 MHz) δ=113.0, 122.9, 126.6, 126.9, 127.6, 128.1, 128.2, 129.2 (s), 131.5, 132.0, 132.7 (s), 134.1, 135.2, 136.7, 142.5(s), 148.0, 183.2 ppm.

MS (m/z): 314.3 (M+1ion peak),

2-(benzo[d]imidazol-2-yl)-1H-phenalen-1-one derivatives from phosphoric acid (7)

A mixture of respective 3-(benzo[*d*]imidazol-2-yl)naphthalen-2-ol (1 g, 1 eq.), p-nitrobenzene sulfonic acid sodium salt (0.86 g, 1 eq.), glycerol (5.21 g, 15 eq.), ferrous sulphate (0.21 g, 0.2 eq.) and boric acid (0.3 g, 1.3 eq.) was heated at 150–155 °C in presence of phosphoric acid (10 mL) for 100 min. Reaction progress was monitored by TLC. After completion of reaction, allowed to cool to room temperature. It was slowly quenched to crushed ice. Final compound was extracted with ethyl acetate. Ethyl acetate layer was dried over sodium sulphate and concentrated to get crude product. Further crude product was recrystallized from ethyl alcohol. Crude yield=59 %, M. P =252-255 °C.

FT-IR 3311 (−N-H stretching), 2923 (Aromatic -CH Stretching), 1725 (C=O stretching) 1577, 1505, 1408, (C=C, C=N ring stretching), 1236, 1110 (C-O stretching), 936, 792, 641 (Aromatic -CH out of plane bending) cm^{-1}.

Table 7 Ground state stability of each conformer of compound **5-10**[a]

Compound No	Energy (K cal mol^{-1})	
	Rotamer a	Rotamer b
5	−611179.4499	−611180.9699
6	−813841.3930	−813855.0692
7	−598714.5566	−598729.1089

[a] TD-DFT computations were carried out with the use of optimized structures at B3LYP method with 6-31G(d) basis set

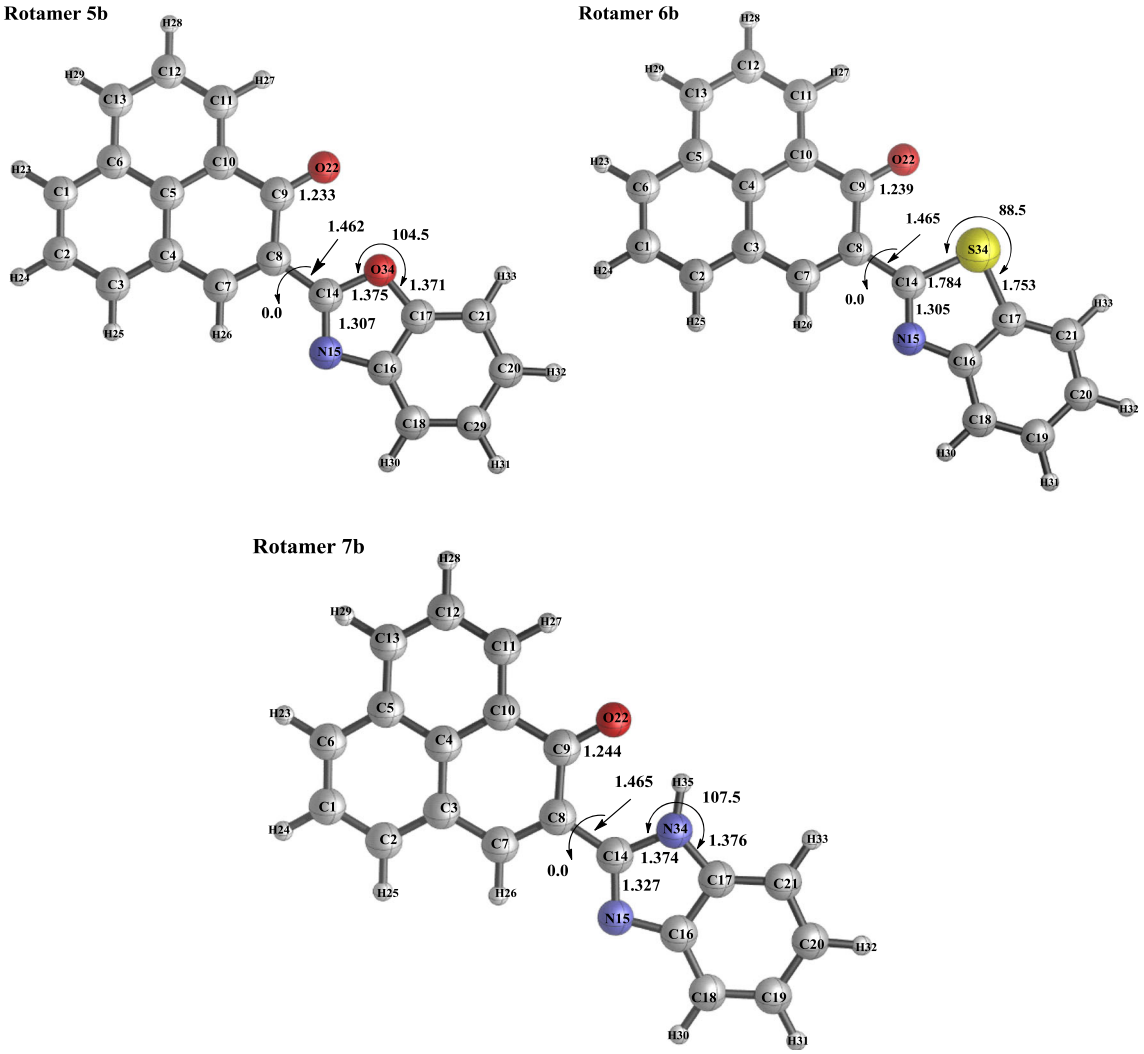

Fig. 9 Optimized structures of compound **5**–**7** in methanol

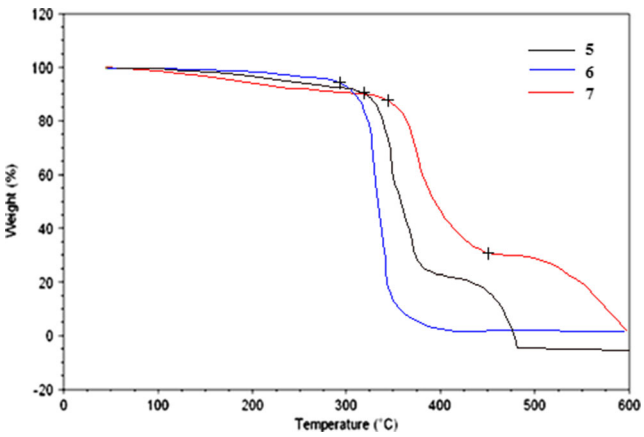

Fig. 10 TGA curves of compound **5**–**7**

^{1}H *NMR* (DMSO-d_6, 300 MHz) δ=7.20-7.23 (m, *J*=1.7, 6.9, 8.1 Hz, 2H, Ar-H), 7.67-7.69 (m, *J*=2.9, 7.9, 8.3 Hz, 2H, Ar-H), 7.83 (t, *J*=1.9, 2.9, 8.1 Hz, 1H, Ar-H), 7.98 (t, *J*=2.6, 8.1 Hz, 1H, Ar-H), 8.03 (t, *J*=1.8, 7.2 Hz, 1H, Ar-H), 8.35 (d, 2.2, 8.1 Hz, 1H, Ar-H). 8.45 (t, *J*=2.5, 7.1 Hz, 1H, Ar-H), 8.57(d, *J*=1.8, 7.8 Hz, 1H, Ar-H), 8.73 (d, *J*=2.0, 7.4 Hz, 1H, Ar-H), 12.70 (s, 1H, −NH) ppm.

MS (m/z): 297.4 (M+1ion peak).

Table 8 Thermal Gravimetric Analysis (TGA) of compound[a]

Compound	TGA (°C)
5	321 (91.43 %)
6	298 (95.78 %)
7	347 (83.80 %)

[a] TGA was measured in °C and measure up to 600 C.

Conclusion

To conclude, in this chapter we have successfully synthesized novel fluorescent 2-(benzo[*d*]azol-2-yl)-1*H*-phenalen-1-one derivatives **5**–**7**. All compounds were well characterized by ^{1}H NMR, ^{13}C NMR and mass spectroscopy. The solvatochromism study for all molecules shows that all shows absorption in the range of 297–462 nm while emits in the range of 391–578 nm. All the three compounds show one λ_{max} and other two shoulder peaks. Compound **6** shows dual emission in all solvents except methanol. For all compounds the vertical excitations were calculated by using TD-DFT technique and all were are in good agreement with the experimental absorption maxima. Exceptionally in compound **5** and **6** the 40–50 nm difference was observed between experimental computed emissions for HOMO-LUMO. The emission intensity continuously decreases as viscosity increases for all compounds. The Thermogravimetric Analysis shows that all the compounds are thermally well stable up to 298–347 °C.

Acknowledgments Kiran Ramnath Phatangare is thankful to UGC-CAS for providing research fellowship under Special Assistance Programme (SAP). Sandip Kisan Lanke is thankful to UGG-CSIR for Senior Research Fellowship (SRF).

References

1. Anamimoghadam O, Symes MD, Busche C, Long DL, Caldwell ST, Flors C, Nonell S, Cronin L, Bucher G (2013) Naphthoxanthenyl, a new stable phenalenyl type radical stabilized by electronic effects. Org Lett 15:2970–2973
2. Nakasuji K, Yamaguchi M, Murata I, Yamaguchi K, Fueno T, Nishiguchi HO, Sugano T, Kinoshita M (1989) Synthesis and characterization of phenalenyl cations, radicals, and anions having donor and acceptor substituents: three redox states of modified odd alternant systems. J Am Chem Soc 111:9265–9267
3. Daza MC, Doerr M, Salzmann S, Marian CM, Thiel W (2009) Photophysics of phenalenone: quantum-mechanical investigation of singlet-triplet intersystem crossing. Phys Chem Chem Phys 11:1688–1696
4. Grabchev I, Philipova T (1998) Synthesis, spectral properties and application of some reactive anthraquinone dyes. Dye Pigment 39: 89–95
5. Stewart WW (1981) Lucifer dyes-highly fluorescent dyes for biological tracing. Nature 292:17–21
6. Chen X, Wang H, Jin X, Fing J, Wang Y, Lu P (2011) Palladium catalyzed bicyclization of 1,8-diiodonaphthalene and tertiary propargylic alcohols to phenalenones and their applications as fluorescent chemosensor for fluoride ions. Chem Commun (Camb) 47: 2628–2630
7. Schmidt R, Tanielian C, Dunsbach R, Wolff C (1994) Phenalenone, a universal reference compound for the determination of quantum yields of singlet oxygen O2(1Δg) sensitization. J Photochem Photobiol A Chem 79:11–17
8. Lorente C, Arzoumanian E, Castaño C, Oliveros E, Thomas AH (2014) A non-singlet oxygen mediated reaction photoinduced by phenalenone, a universal reference for singlet oxygen sensitization. RSC Adv 4:10718–10727
9. Martí C, Jürgens O, Cuenca O, Casals M, Nonell S (1996) Aromatic ketones as standards for singlet molecular oxygen O2(1Δg) photosensitization time-resolved photoacoustic and near-IR emission studies. J Photochem Photobiol A Chem 97:11–18
10. Ragàs X, Jiménez-Banzo A, Sánchez-García D, Batllori X, Nonell S (2009) Singlet oxygen photosensitisation by the fluorescent probe singlet oxygen sensor. Green Chem Commun (Camb) 2920–2922
11. Flors C, Nonell S (2006) Light and singlet oxygen in plant defense against pathogens: phototoxic phenalenone phytoalexins. Acc Chem Res 39:293–300
12. Kamo T, Hirai N, Iwami K, Fujioka D, Ohigashi H (2001) New phenylphenalenones from banana fruit. Tetrahedron 57:7649–7656
13. Opitz S, Otálvaro F, Echeverri F, Quinones W, Schneider B (2002) Isomeric oxabenzochrysenones from musa acuminata and wachendorfia thyrsiflora. Nat Prod Lett 16:335–338
14. Flors C, Nonell S (2004) Radical species derived from phenalenone: characterization and role of upper excited states. J Photochem Photobiol A Chem 163:9–12
15. Kunavich NI, Shamraev VN, Solodar' SL (1986) Electronic spectra and structure of molecules of phenalenone and its 6-methoxy- and 6-dimethylamino derivatives. J Appl Spectrosc 45:967–970
16. Phatangare KR, Gupta VD, Tathe AB, Padalkar VS, Patil VS, Ramasami P, Sekar N (2013) ESIPT inspired fluorescent 2-(4-benzo[d]oxazol-2-yl)naphtho[1,2-d]oxazol-2-yl)phenol: experimental and DFT based approach to photophysical properties. Tetrahedron 69:1767–1777
17. Phatangare KR, Lanke SK, Sekar N (2014) Fluorescent coumarin derivatives with viscosity sensitive emission - synthesis, photophysical properties and computational studies. J Fluoresc 24: 1263–1274
18. Ueno R, Kitayama Y, Minami K, Wakamori H (2004) Binaphthol derivative and process for producing the same
19. Matsui K, Kuroda T (1967) Azo dyes derived from 3-(2-benzimidazolyl)-2-naphthol and 3-(2-benzoxazolyl)-2-naphthol. J Soc Chem Ind Japan 70:2325–2329
20. Anthony K, Brown RG, Hepworth JD, Hodgson KW, May B, West MA (1984) Solid-state fluorescent photophysics of some 2-substituted benzothiazoles. J. Chem. Soc. Perkin Trans. 2 2111–2117
21. Douhal A, Amat-Guerri F, Acuña AU, Yoshihara K (1994) Picosecond vibrational relaxation in the excited-state proton-transfer of 2-(3′-hydroxy-2′-naphthyl)benzimidazole. Chem Phys Lett 217: 619–625
22. Fieser LF, Hershberg EB (1938) A New Synthesis of 3,4-Benzpyrene Derivatives. J Am Chem Soc 60:1658–1665
23. Fieser LF, Newton LW (1942) Reactions of Perinaphthane Derivatives. J Am Chem Soc 64:917–921
24. Patil VS, Padalkar VS, Phatangare KR, Gupta VD, Umape PG, Sekar N (2011) Synthesis of new ESIPT-fluorescein: photophysics of pH sensitivity and fluorescence. J Phys Chem A 116:536–545
25. Treutler O, Ahlrichs R (1995) Efficient molecular numerical integration schemes. J Chem Phys 102:346–354
26. Becke AD (1993) A new mixing of Hartree–Fock and local density functional theories. J Chem Phys 98:1372–1377
27. Lee C, Yang W, Parr RG (1988) Development of the colle-salvetti correlation-energy formula into a functional of the electron density. Phys Rev B 37:785–789
28. Kim CH, Park J, Seo J, Park SY, Joo T (2010) Excited state intramolecular proton transfer and charge transfer dynamics of a 2-(2′-hydroxyphenyl)benzoxazole derivative in solution. J Phys Chem A 114:5618–5629
29. Casida ME, Jamorski C, Casida KC, Salahub DR (1998) Molecular excitation energies to high-lying bound states from time-dependent density-functional response theory: Characterization and correction of the time-dependent local density approximation ionization threshold. J Chem Phys 108:4439–4449

30. Bauernschmitt R, Ahlrichs R (1996) Treatment of electronic excitations within the adiabatic approximation of time dependent density functional theory. Chem Phys Lett 256:454–464
31. Hehre WJ, Radom L, Schleyer PV, Pople J (1986) Ab initio molecular orbital theory. Wiley, New York
32. Furche F, Rappaport D (2005) Density functional theory for excited states: Equilibrium structure and electronic spectra. In: Olivucci M (ed) Comput Photochem Elsevier: Amsterdam 93–128
33. Lakowicz JR (1999) Principles of Fluorescence Spectroscopy, 2nd edn. New York, Kluwer Academic
34. Tomasi J, Mennucci B, Cammi R (2005) Quantum mechanical continuum solvation models. Chem Rev 105:2999–3093
35. Cossi M, Barone V, Cammi R, Tomasi J (1996) Ab initio study of solvated molecules: a new implementation of the polarizable continuum model. Chem Phys Lett 255:327–335
36. Frisch MJ, Trucks GW, Schlegel HB Scuseria GE, Robb MA, Cheeseman JR, Scalmani G, Barone V, Mennucci B, Petersson GA, Nakatsuji H, Caricato M, Li X, Hratchian HP, Izmaylov AF, Bloino J, Zheng G, Sonnenberg JL, Hada M, Ehara M, Toyota K, Fukuda R, Hasegawa J, Ishida M, Nakajima T, Honda Y, Kitao O, Nakai H, Vreven T, Montgomery JA Jr, Peralta JE, Ogliaro F, Bearpark M, Heyd JJ, Brothers E, Kudin KN, Staroverov VN, Kobayashi R, Normand J, Raghavachari K, Rendel, A, Burant JC, Iyengar SS, Tomasi J, Cossi M, Rega N, Millam MJ, Klene M, Knox JE, Cross JB, Bakken V, Adamo C, Jaramillo J, Gomperts R, Stratmann RE, Yazyev O, Austin AJ, Cammi R, Pomelli C, Ochterski, JW, Martin RL, Morokuma K, Zakrzewski VG, Voth GA, Salvador P, Dannenberg JJ, Dapprich S, Daniels AD, Farkas Ö, Foresman JB, Ortiz JV, Cioslowski J, Fox DJ (2009) Gaussian 09, Revision C.01. Gaussian 09, Revis B01, Gaussian, Inc, Wallingford CT